JMEPEG (2012) 21:388–394
DOI: 10.1007/s11665-011-9927-y

1059-9495/$19.00

An Investigation on Low-Temperature Thermochemical Treatments of Austenitic Stainless Steel in Fluidized Bed Furnace

E. Haruman, Y. Sun, A. Triwiyanto, Y.H.P. Manurung, and E.Y. Adesta

(Submitted June 15, 2010; in revised form February 1, 2011)

In this study, the feasibility of using an industrial fluidized bed furnace to perform low-temperature thermochemical treatments of austenitic stainless steels has been studied, with the aim to produce expanded austenite layers with combined wear and corrosion resistance, similar to those achievable by plasma and gaseous processes. Several low-temperature thermochemical treatments were studied, including nitriding, carburizing, combined nitriding-carburizing (hybrid treatment), and sequential carburizing and nitriding. The results demonstrate that it is feasible to produce expanded austenite layers on the investigated austenitic stainless steel by the fluidized bed heat treatment technique, thus widening the application window for the novel low-temperature processes. The results also demonstrate that the fluidized bed furnace is the most effective for performing the hybrid treatment, which involves the simultaneous incorporation of nitrogen and carbon together into the surface region of the component in nitrogen- and carbon-containing atmospheres. Such hybrid treatment produces a thicker and harder layer than the other three processes investigated.

Keywords carbon, expanded austenite, fluidized bed furnace, nitrogen, stainless steel

1. Introduction

Austenitic stainless steels are the most popular materials in the stainless steel family used in various applications due to their excellent corrosion resistance and good forming characteristics. Nevertheless, this type of materials has low hardness as well as poor wear resistance due to the inherent austenitic structure. To overcome this problem, efforts have been made in the past decades to modify the surfaces of these materials so as to improve their surface hardness and wear resistance. Nitriding treatment was proposed by various investigators (Ref 1-5), but problems arise due to the sensitization effect caused by the formation of chromium nitrides when these materials are treated at a nitriding temperature above 500 °C (Ref 1). Early investigations in the mid of 1980s suggested that applying low-temperature nitriding would suppress the formation of chromium nitrides and produce a thin nitrided layer with high hardness and acceptable corrosion resistance (Ref 2, 3). Since then, significant progress has been made toward achieving combined improvements in wear and corrosion resistance of austenitic stainless steels by low-temperature thermochemical treatments (Ref 4, 6).

The two major low-temperature thermochemical processes developed for austenitic stainless steels are nitriding and carburizing (Ref 4, 7). The former is normally carried out at temperatures below 450 °C and the later below 500 °C. The purpose of using low temperatures is to suppress the formation of chromium nitrides and carbides in the alloyed layers, such that chromium is retained in solid solution for corrosion protection (Ref 5, 8). Hardening of the nitrided layer and the carburized layer is due to the incorporation of nitrogen and carbon, respectively, in the austenite lattice, forming a structure termed expanded austenite, which is supersaturated with nitrogen and carbon, respectively (Ref 7, 9). More recently, a hybrid process has also been developed, which combines the nitriding and carburizing actions in a single process cycle by introducing nitrogen and carbon simultaneously into the austenite lattice to form a hardened zone comprising a nitrogen expanded austenite layer on top of a carbon expanded austenite layer (Ref 10-12). There exist some synergetic effects between nitrogen and carbon: Under similar processing conditions, the hybrid-treated layer is thicker, harder, and possesses better corrosion resistance than the individual nitrided layer and carburized layer.

The most popular technology used to achieve the aforementioned low-temperature thermochemical treatments of stainless steels is plasma technology, namely plasma nitriding (Ref 6, 13), plasma carburizing (Ref 14, 15), and plasma hybrid treatments (Ref 11, 12). Due to the formation of a native oxide film on stainless steel surface when exposed to air or residual oxygen before and during the treatment process, it is rather difficult to facilitate nitrogen and carbon mass transfer from the

E. Haruman and **Y.H.P. Manurung**, Fakulti Kejuruteraan Mekanikal, Universiti Teknologi Mara, 40450 Shah Alam, Malaysia; **Y. Sun**, School of Engineering and Technology, De Montfort University, Leicester LE19BH, UK; **A. Triwiyanto**, Department of Mechanical Engineering, Universiti Teknologi PETRONAS, 31750 Tronoh, Malaysia; and **E.Y. Adesta**, Department of Manufacturing and Materials Engineering, Kulliyyah of Engineering, International Islamic University Malaysia, 50728 Kuala Lumpur, Malaysia. Contact e-mails: esa@salam.uitm.edu.my and rez_mana@yahoo.com.

treatment media to the component surface. However, during plasma processing, due to the sputtering effects of energetic ions, the oxide film can be removed easily and effective mass transfer is obtained. This makes the plasma technology unique for surface treatment of stainless steels. An alternative is using the more conventional gaseous processes like gas nitriding (Ref 16) and gas carburizing (Ref 17). These have proven feasible and industrially acceptable for performing low-temperature nitriding and carburizing of stainless steels, provided that the component surface is activated before the gaseous process by special chemical treatments and the oxide film formed during the gaseous process is disrupted by introducing certain special gas components (Ref 16).

Fluidized bed technology is being increasingly used in the heat treatment industry, due to the increased energy efficiency, more uniform temperature, and reduced treatment time achievable in a fluidized bed furnace (Ref 18, 19). Indeed, nitriding and nitrocarburizing are now commonly performed in fluidized bed furnaces for surface hardening of engineering steel components (Ref 18). However, very few efforts have been made to produce expanded austenite layers on austenitic stainless steels in a fluidized bed furnace by employing the low-temperature techniques. Recent study by the present authors has demonstrated that a nitrogen expanded austenite layer can be formed on 316L austenitic stainless steel in a fluidized bed furnace by low-temperature nitriding (Ref 20). Further research has since been conducted to study the possibility of forming a carburized layer and a combined nitrided and carburized layer by the low-temperature carburizing and hybrid processes in a fluidized bed furnace, with the aim of widening the application window for the low-temperature technology. This article reports the experimental results obtained and describes the characteristics of 316L steel treated at 450 °C and for 8 h duration.

2. Experimental

The material used in this study is AISI316L austenitic stainless steel with the following nominal chemical compositions (in wt.%): 17.018 Cr, 10.045 Ni, 2.00 Mo, 1.53 Mn, 0.03 C, 0.048 Si, 0.084 P, 0.03 S, and balance Fe. The material was received in the form of a hot-rolled plate and was machined into test specimens of $20 \times 20 \times 2$ mm^3 sizes. Prior to the treatments, the sample surface was ground and polished to 1 μm surface finish (R_a) and soaked into concentrated HCl (2 M) solution to remove the native oxide film on the surface. The treatments were performed at 450 °C for a total duration of 8 h in an electrical resistance heated fluidized bed furnace having 105 μm particulate alumina as fluidized particles which flow inside the chamber due to the flow of nitriding or carburizing gases. The fluidized bed furnace, which was manufactured by Quality Heat Technologies Pty Ltd (Melbourne, Australia) has a working chamber of 100 mm diameter × 250 mm deep with maximum worksize of 70 mm diameter × 150 mm high. Before charging the samples, the chamber was heated to the treatment temperature of 450 °C with the flow of nitrogen gas at 1.05 m^3/h. Then the samples were charged to the furnace and the treatment gases were introduced and their flow rates were adjusted to meet the required composition, with the total gas flow rate maintained at 0.62 m^3/h. Table 1 summarizes the process conditions employed in this study. Four different

Table 1 Treatment conditions and corresponding layer thicknesses

			Gas, %			Gas, %		
Treament	**Time, h**	**Temp, °C**	**CH_4**	**N_2**	**NH_3**	**CH_4**	**N_2**	**NH_3**
Nitriding	8	450	…	85	15	…	…	…
Carburizing	8	450	5	95	…	…	…	…
Hybrid process	8	450	5	80	15	…	…	…
			1st step (C)			**2nd step (N)**		
Carburizing + nitrding	4 + 4	450	5	95	…	…	85	15

treatments were conducted, including low temperature nitriding, carburizing, hybrid process, and sequential carburizing-nitriding. The hybrid process involved treating the sample in an atmosphere containing both NH_3 (for nitriding) and CH_4 (for carburizing) for a total duration of 8 h, while the sequential process involved treating the sample in the carburizing atmosphere for 4 h and then in the nitriding atmosphere for further 4 h.

After the treatments, the structure and morphology of the treated specimens were characterized using scanning electron microscope (SEM). The hybrid-treated specimen was also characterized by scanning probe microscope (SPM 9600 Shimadzu) to reveal 3D surface topographical profile at higher resolutions. To obtain the topographical profile of the specimen, the contact mode was applied with 1.2 V constant operating force, 1 Hz scanning rate, 0.1 μm Z-axis range, for both 1×1 μm top surface and 5×5 μm cross-sectional cut. Microhardness profiles across the resultant alloyed layers were measured by micro-Vickers hardness testing with an indentation load of 50 g. Elemental profile of carbon across the hybrid treated layers was obtained by EDS-SEM to reveal the push-in effect of dissolved carbon by nitrogen. X-ray diffraction (XRD) analysis using Cu-Kα radiation (40 kV, 150 mA) was performed to identify the phase composition in the treated layers under various process conditions. Tribological behaviors were evaluated with a Taber R Linear model 5750 dry slide tribotester using a 5 mm diameter AISI 316L collet nut as mate material. The stroke length applied was 25.4 mm under a constant load 600 g. After 3600 cycles of sliding (completed in 60 min) having maximum velocity of 79.76 mm/s, the specimen's wear loss was measured by balance to evaluate cumulative weight loss.

3. Results and Discussion

3.1 Layer Morphology

The morphology of the hardened layers resulting from various treatments is shown in Fig. 1. Clearly, nitriding in the fluidized bed resulted in the formation of a single layer, presumably nitrogen expanded austenite (γ_N), on the surface (Fig 1a). This confirms the results reported earlier (Ref 20). More importantly, this study demonstrates that the fluidized bed furnace can also be used to successfully perform low-temperature carburizing, as can be seen from Fig. 1(b), which shows that a single carburized layer comprising carbon expanded

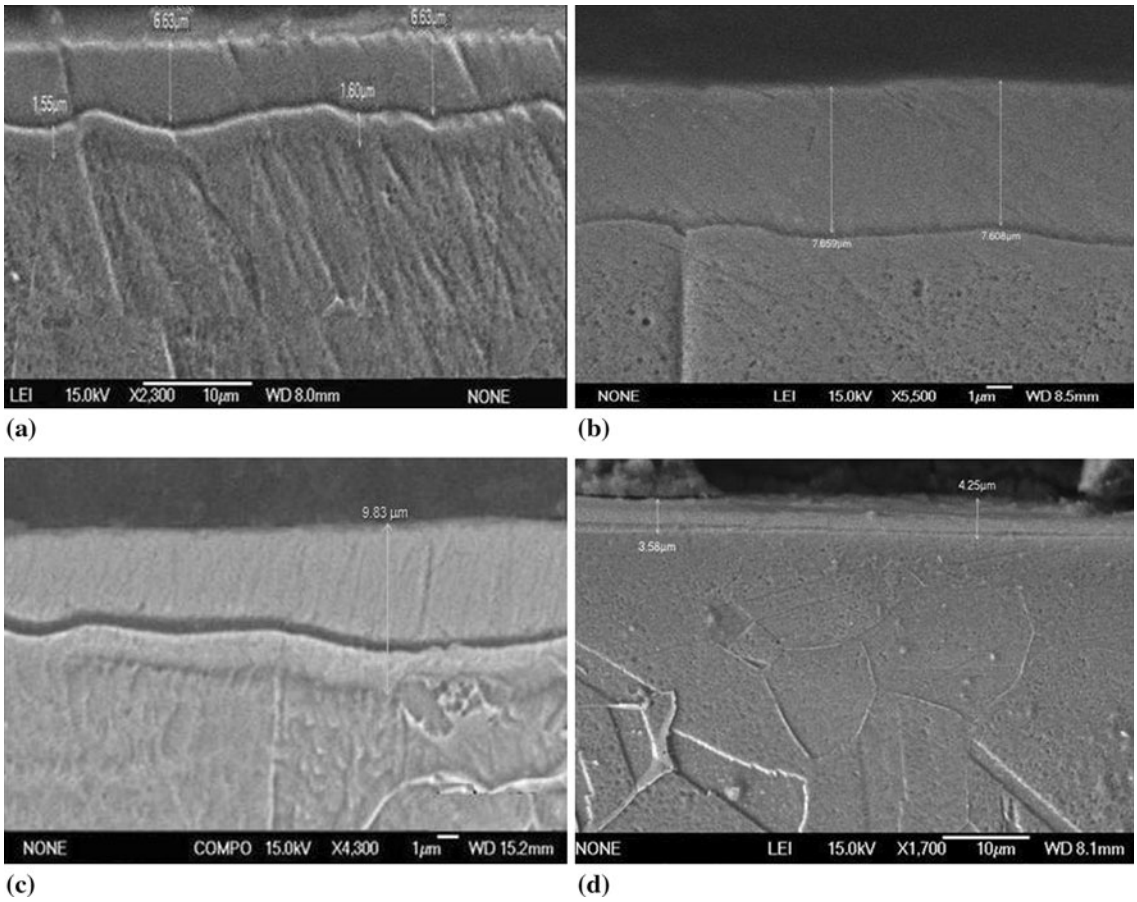

Fig. 1 SEM micrographs of 450 °C treated specimens: (a) nitrided 8 h, (b) carburized 8 h, (c) hybrid-treated 8 h, (d) sequential: 4 h carburized + 4 h nitrided

austenite (γ_C) was formed on the surface (see XRD patterns in Fig. 5).

As expected, the hybrid treatment resulted in the formation of a dual layer structure with a thick nitrogen expanded austenite (γ_N) occupying the outer layer zone and a thinner carbon expanded austenite (γ_C) occupying the inner layer zone (Fig. 1c). Although not clearly revealed in the present micrograph, this separation of dual structure is observable under optical microscope. The carbon profile across the hybrid dual layers is given in Fig. 2. A high carbon peak was detected at the inner layer, thus proving the push-in effect of dissolved carbon by nitrogen during the hybrid process. The results from the fluidized bed hybrid treatment are similar to those reported for plasma hybrid treatments (Ref 11, 12). The formation of a dual layer structure is obviously the result of the simultaneous introduction of nitriding species and carbon species in the treatment atmosphere. The carbon species possess greater diffusivity and would penetrate further into the substrate than nitrogen (Ref 11). Since both carbon and nitrogen occupy the same kind of interstitial sites in the fcc lattice, the arrival of the slower diffusing nitrogen atoms would force the carbon atoms (the early comer) to make available the interstitial sites. The only easy path for carbon is to diffuse further into the substrate, thus forming a push-in effect of carbon by nitrogen and a separate carbon expanded austenite layer. Surface topography of the hybrid-treated specimen obtained by SPM is given in Fig. 3(a). It can be seen that the treated surface is populated with globular features of nanometer scale in size, similar to the

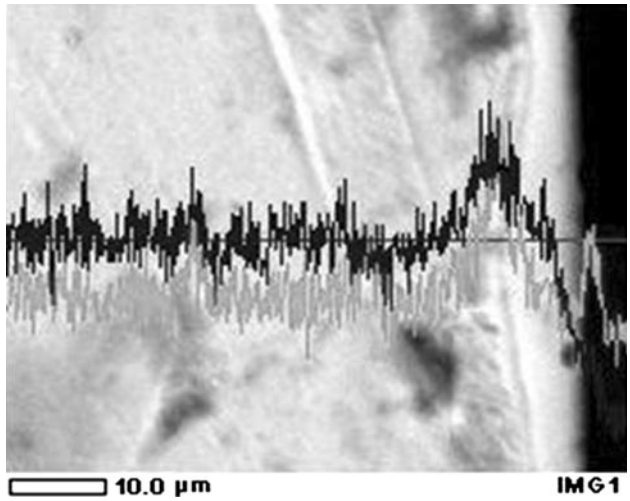

Fig. 2 Carbon peak at the bottom part of the hybrid-treated layer, as revealed by EDS line scanning

morphological features observed from plasma hybrid-treated surface (Ref 11). SPM examination of the cross section revealed further details that have not been noticed before (Fig. 3b). The dual layer structure is clearly seen in Fig. 3(b), which also reveals the columnar growth of the two sublayers as a result of nitrogen and carbon diffusion. The densely packed columnar structure of the two expanded austenite layers

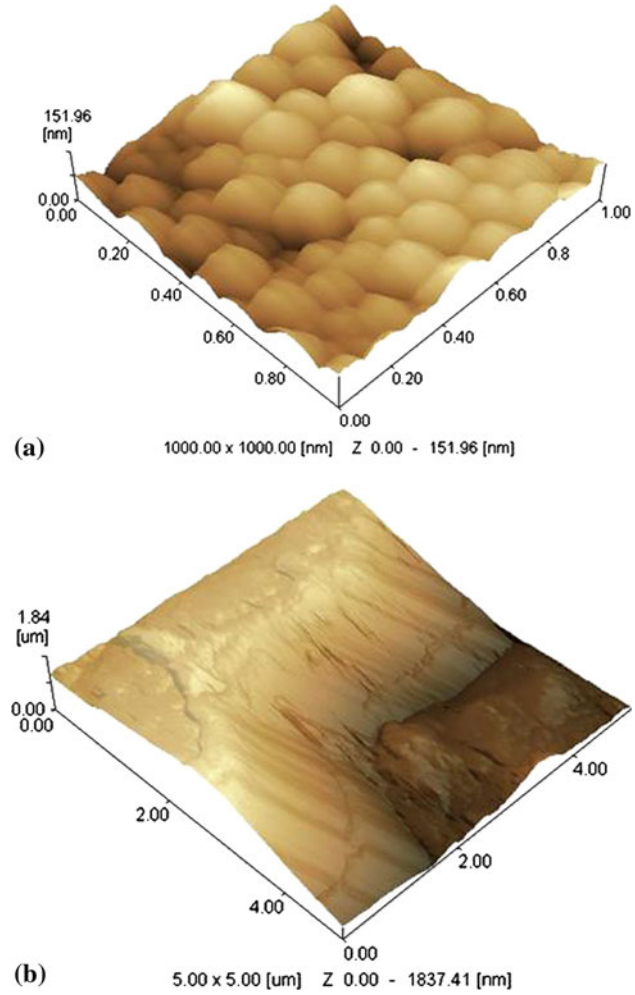

Fig. 3 SPM images showing (a) 3D surface morphology of expanded austenite layer from top view, and (b) cross-sectional view of the hybrid-treated layer

correlates well with the globular surface structure observed in Fig. 3(a).

Rather surprisingly, the sequential carburizing-nitriding treatment did not result in the formation of a dual layer structure, but only a thin single layer (Fig. 1d). XRD analysis discussed later showed that this single layer comprises carbon expanded austenite. Thus, nitrogen expanded austenite failed to develop during the sequential treatment. This observation is different from that found during plasma processing. For example, Tsujikawa et. al. (Ref 10) conducted sequential carburizing-nitriding treatment of 316L stainless steel and found the formation of a duplex layer structure. The absence of a dual layer structure by the fluidized bed sequential treatment is likely due to the fact that transfer of nitrogen and carbon in fluidized bed furnace is solely controlled by thermal decomposition of ammonia and hydrocarbon gas on the austenitic stainless steel surface.

3.2 Layer Thickness

The layer thicknesses are also found to be different for different treatments. In this study, at a constant temperature of 450 °C and for 8 h duration, the hybrid process produced a

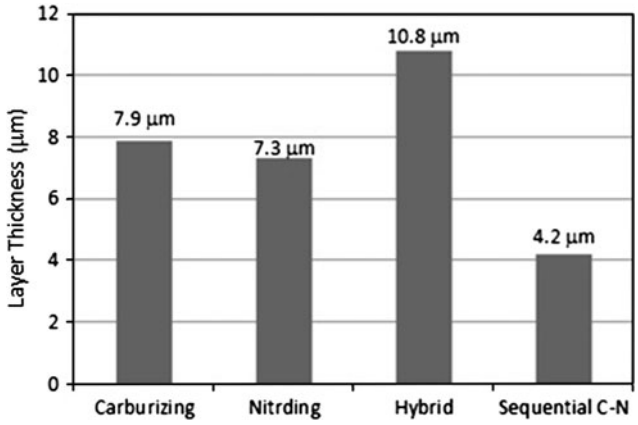

Fig. 4 Layer thickness of expanded austenite layers resulting from low-temperature treatments

larger layer thickness than those produced by nitriding, carburizing, and sequential carburizing-nitriding (Fig. 4), confirming the synergy between carbon and nitrogen. However, such synergetic effect was found only when nitrogen and carbon are introduced simultaneously. This study shows that introducing sequential carbon and nitrogen diffusion (in the sequential carburizing-nitriding treatment) did not result in similar layer characteristics compared to the layer produced by simultaneous carbon and nitrogen diffusion in the hybrid process. The resultant layer thickness produced by sequential carburizing-nitriding is much smaller than the layer thickness produced by the hybrid process, and is even smaller than that produced by individual carburizing and nitriding. Despite the lack of measured data, this phenomenon could be explained as follows. The first step of the process, carburizing for 4 h, would produce a carburized layer with carbon atoms occupying the interstitial sites of the fcc lattice in the surface region. When the second step, i.e., nitriding commenced after 4 h, the carburizing effect ceased and the diffusion of nitrogen became sluggish in the carbon expanded austenite layer already formed in the previous carburizing cycle. The push-in effect still prevailed, which would lead to the formation of a dual layer structure. But since there was no more carbon supply during the nitriding cycle, the carbon atoms pushed to the nitriding front still continued to diffuse into the substrate, leading to the gradual leveling off of the carbon concentration and thus the diminish of the carburized layer. Other possibility could be due to the decarburization of the carburized layer during the early stage of the subsequent nitriding cycle, which would lead to a reduction in the carbon expanded austenite (γ_N) layer thickness. In addition, since the nitrided layer was allowed to grow for only 4 h, a thinner layer thickness is expected than that produced by individual nitriding for 8 h.

The greater thickness of the dual layer resulting from hybrid process can be explained by the enhanced thermodynamic activities (a_C, a_N) of both diffusing carbon and nitrogen in the alloyed zone during the treatment, a situation similar to conventional carbonitriding of low alloy steels at temperatures around 850 °C (Ref 21). In addition, some carbon-nitrogen radicals (CN_x) would possibly form in the treatment atmosphere, which have a high reducing power to reduce the surface oxide film on the specimen surface, thus promoting nitrogen and carbon mass transfer during the hybrid process.

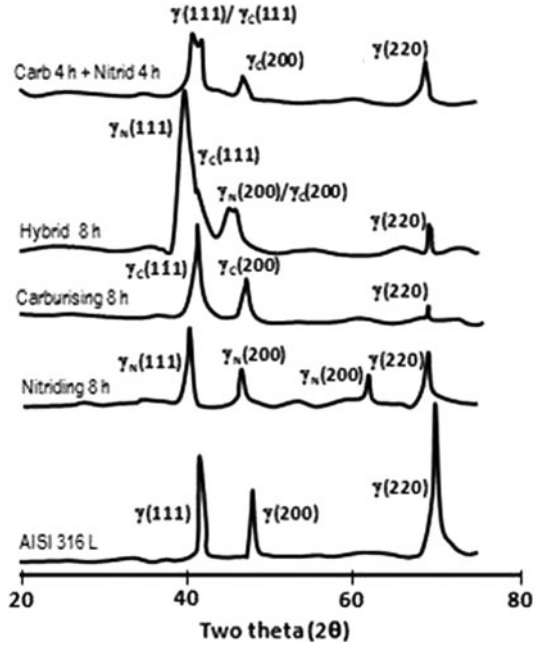

Fig. 5 XRD patterns of various low-temperature-treated surfaces showing the formation of γ_N and/or γ_C, and the absence of nitride and carbide precipitates

3.3 XRD Analysis

XRD analysis (Fig. 5) confirmed the phase composition and layer structure discussed in section 3.1 for various resultant layers. In all the resultant layers, no nitride and carbide precipitates were detectable by XRD. This is in close agreement with previous results (Ref 5, 9, 17) on individual plasma nitriding and carburizing which conclude that the formation of nitride and carbide precipitates requires a higher temperature, and the temperature of 450 °C does not favor the formation of these precipitates. Thermodynamically, chromium nitrides and carbides could form under this process condition, however, at this relatively low processing temperature; the rate of precipitation is sluggish such that for a short treatment period the produced nitrided and carburized layers are precipitation-free. The significant amount of carbon or nitrogen dissolved in the layer obviously leads to the supersaturation of the austenite lattices (Ref 4). The austenite lattice in the surface alloyed layer is expanded as evidenced from the shift of the XRD peaks to lower diffraction angles as compared to the corresponding peaks from the untreated substrate. According to the XRD results, a lattice expansion by 9% was found for the γ_N phase and 3% for the γ_C phase in this study. These lattice expansions on expanded austenite were calculated from XRD peak shift which was developed by previous study (Ref 22). In this investigation, however, a calculation of lattice expansion correlated to carbon/nitrogen content was not performed because of the lack of quantification of C/N concentration by EDS.

3.4 Hardness Profile

Hardness profile measurements across each of the resultant layers confirm the hardening effect of the low-temperature thermochemical treatments. As can be seen from Fig. 6, the sequential carburizing-nitriding treatment resulted in the smallest hardened layer thickness, and the individual carburized layer exhibits the lowest surface hardness (but still as high as 1200 $HV_{0.05}$) but a gradually decreased hardness gradient. On the other hand, the individual nitrided layer exhibits much higher hardness than the carburized layer, but with a more abrupt drop in hardness at the layer/core interface. The hybrid layer possesses the most favorable hardness distribution: the surface hardness is as high as that of the individual nitride layer, and the hardness decreases gradually toward the layer/core interface. Such a gentle hardness gradient in the dual layer from hybrid process is expected to be beneficial in achieving enhanced tribological and load bearing properties (Ref 9, 11).

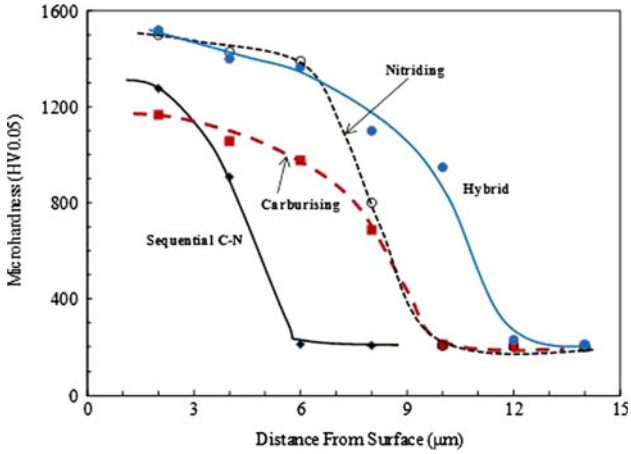

Fig. 6 Hardness profiles measured across the hardened layers resulting from various treatment conditions

It is worthwhile to point out that under similar processing temperature and time conditions, plasma processes produce much thicker layers than those produced by the present treatments in fluidized bed furnace. In plasma processes, the native oxide film is removed mostly by bombardment of the positive charged particles, which is completely absent in conventional fluidized processes. Thermal decomposition and mechanical impinging by flowing alumina particulates are believed to be the mechanisms responsible for disruption of the surface oxide film during fluidized processes. Further efforts are required to optimize the fluidized processes so as to achieve much accelerated mass transfer and layer growth kinetics. Despite this limitation, the fluidized bed processes have several advantages over plasma processes, such as: low investment cost, temperature uniformity due to agitation effect by bed particles, and low production cost. These factors make the fluidized the bed process have gained industrial acceptance in heat treatment industries.

3.5 Wear Properties

Wear test results presented in Fig. 7 correlate well with the hardness test results in Fig. 6 and confirm the improvement in wear resistance of the specimens after the treatments in the fluidized bed furnace. The hybrid-treated specimens and nitrided specimens exhibited the lowest cumulative wear loss, followed by carburized specimens. In the case of sequential (C-N)-treated specimens the improvement, however, is insignificant. The poor wear resistance of this specimen seems to be correlated with its thin layer formation (4.3 μm) and its ragged surface morphology (Fig. 1). Thus, during dry slide wear the

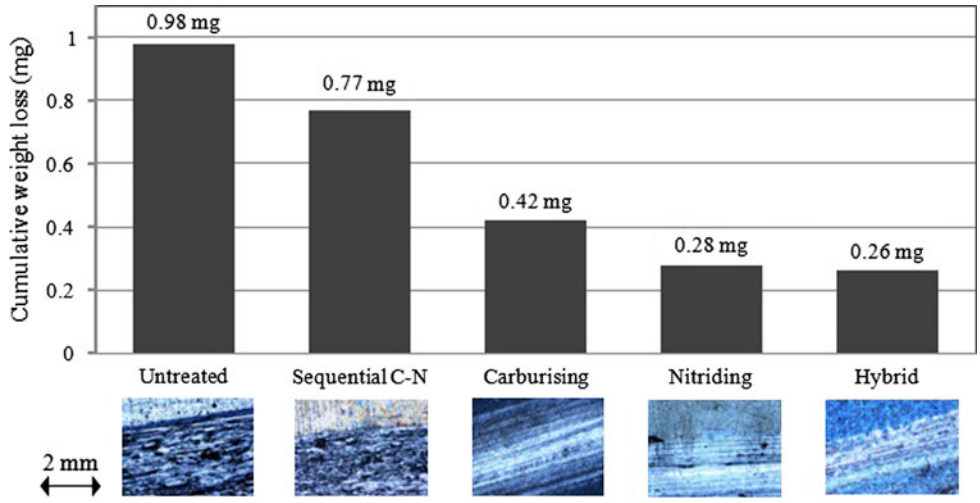

Fig. 7 Wear test results on various low-temperature thermochemical-treated AISI 316L steel

hard debris resulting from detachments of contacting asperities would further penetrate the specimen surface leading to a severe wear phenomenon as can be seen from wear track images in Fig. 7. This tendency did not occur with the specimens treated by carburization, nitriding, and hybrid processes which possessed significantly larger thickness and higher hardness of the layer (Table 1). The wear track surfaces of these specimens are smooth with some abrasive marks, but with no sign of plastic deformation and delamination as can be seen from the images in Fig. 7. Although a further investigation is required to study the effect of layer thickness and surface hardness on wear behavior, the wear test results have evidently shown improvements in wear resistance of AISI 316L after low-temperature thermochemical treatments in fluidized furnace.

4. Conclusions

This study demonstrates that it is feasible to produce expanded austenite layers on the investigated austenitic stainless steel by the fluidized bed processes, thus widening the application window for the novel low-temperature processes. The expanded austenite layers resulting from the fluidized bed processes have similar characteristics to those produced by plasma processes. But the layers produced by the fluidized processes are thinner than those produced by plasma processes, due to different mass transfer mechanisms. The results also demonstrate that the fluidized bed furnace is the most effective for performing the hybrid treatment, which involves the simultaneous incorporation of nitrogen and carbon together into the surface region of the component in nitrogen- and carbon-containing atmospheres. Such hybrid treatment produces a thicker and harder layer than the other three processes investigated.

Acknowledgments

The authors would like to thank Faculty of Mechanical Engineering, Institute of Technology National Malang, Indonesia, for the provision of fluidized bed heat treatment furnace to enable the present work to be completed.

References

1. E. Rolinski, Effect of Plasma Nitriding Temperature on Surface Properties of Austenitic Stainless Steel, *Surf. Eng.*, 1987, **3**, p 35–40
2. K. Ichii, K. Fujimura, and T. Takase, Structure of the Ion-Nitrided Layer of 18-8 Stainless Steel, *Tech. Rep. Kansai Univ.*, 1986, **27**, p 135–144
3. Z.L. Zhang and T. Bell, Structure and Corrosion Resistance of Plasma Nitrided Stainless Steel, *Surf. Eng.*, 1985, **1**, p 131–136
4. T. Bell and Y. Sun, Low Temperature Plasma Nitriding and Carburising of Austenitic Stainless Steels, *Heat Treat. Met.*, 2002, **29**(3), p 57–64
5. Y. Sun, X.Y. Li, and T. Bell, X-ray Diffraction Characterisation of Low Temperature Plasma Nitrided Austenitic Stainless Steels, *J. Mater. Sci.*, 1999, **34**, p 4793–4802
6. K.-T. Rie and E. Broszeit, Plasma Diffusion Treatment and Duplex Treatment—Recent Development and New Applications, *Surf. Coat. Technol.*, 1995, **76–77**, p 425–436
7. D.B. Lewis, A. Leyland, P.R. Stevenson, J. Cawley, and A. Matthews, Metallurgical Study of Low Temperature Plasma Carbon Diffusion Treatments for Stainless Steels, *Surf. Coat. Technol.*, 1993, **60**, p 416–423
8. Y. Sun, X.Y. Li, and T. Bell, Low Temperature Plasma Carburising of Austenitic Stainless Steels for Improved Wear and Corrosion Resistance, *Surf. Eng.*, 1999, **15**, p 49–54
9. S. Thaiwatthana, X.Y. Li, H. Dong, and T. Bell, Mechanical and Chemical Properties of Low Temperature Plasma Surface Alloyed 316 Austenitic Stainless Steel, *Surf. Eng.*, 2002, **18**, p 140–144
10. M. Tsujikawa, D. Yoshida, N. Yamauchi, N. Ueda, T. Sone, and S. Tanaka, Surface Material Design of 316 Stainless Steel by Combination of Low Temperature Carburizing and Nitriding, *Surf. Coat. Technol.*, 2005, **200**, p 507–511
11. Y. Sun and E. Haruman, Influence of Processing Conditions on Structural Characteristics of Hybrid Plasma Surface Alloyed Austenitic Stainless Steel, *Surf. Coat. Technol.*, 2008, **202**, p 4069–4075
12. X.Y. Li, J. Buhagiar, and H. Dong, Characterisation of Dual S Phase Layer on Plasma Carbonitrided Biomedical Austenitic Stainless Steels, *Surf. Eng.*, 2010, **26**, p 67–73
13. J.C. Stinville, P. Villechaise, C. Templier, J.P. Riviere, and M. Drouet, Plasma Nitriding of 316L Austenitic Stainless Steel: Experimental Investigation of Fatigue Life and Surface Evolution, *Surf. Coat. Technol.*, 2010, **204**, p 1947–1951
14. Y. Sun, Kinetics of Low Temperature Plasma Carburizing of Austenitic Stainless Steels, *J. Mater. Process. Technol.*, 2005, **168**, p 189–194
15. M. Tsujikawa, S. Noguchi, N. Yamauchi, N. Ueda, and T. Sone, Effect of Molybdenum on Hardness of Low-Temperature Plasma Carburized Austenitic Stainless Steel, *Surf. Coat. Technol.*, 2007, **201**, p 5102–5107

16. K. Gemma, T. Obtruka, T. Fujiwara, and M. Kwakami, Prospects for Rapid Nitriding in High Cr Austenitic Alloys, *Stainless Steel 2000*, T. Bell and K. Akamatsu, Ed., Maney Publishing, Leeds, 2001, p 159–166
17. F. Ernst, Y. Cao, G.M. Michal, and A.H. Heuer, Carbide Precipitation in Austenitic Stainless Steel Carburized at Low Temperature, *Acta Mater.*, 2007, **55**, p 1895–1906
18. W.M. Gao, L.X. Kong, and P.D. Hodgson, Numerical Simulation of Heat and Mass Transfer in Fluidised Bed Heat Treatment Furnaces, *J. Mater. Process. Technol.*, 2002, **125–126**, p 170–178
19. A. Türk, Ok Orcun, and C. Bindal, Structural Characterization of Fluidized Bed Nitrided Steels, *Vacuum*, 2005, **80**, p 332–342
20. E. Haruman, Y. Sun, H. Malik, and S. Mridha, Low Temperature Fluidized Bed Nitriding of Austenitic Stainless Steel, *Solid State Phenom.*, 2006, **118**, p 125–130
21. K.H. Prabhudev, *Handbook of Heat Treatment of Steels*, Tata McGraw-Hill Publishing, Delhi, 1999
22. O. Öztürk and D.L. Williamson, Phase and Composition Distribution Analyses of Low Energy High Flux N Implanted Stainless Steels, *J. Appl. Phys.*, 1995, **77**, p 3839–3851